

In situ nanocalorimetry of thin glassy organic films

Cite as: J. Chem. Phys. **129**, 181101 (2008); <https://doi.org/10.1063/1.3009766>

Submitted: 15 July 2008 . Accepted: 09 October 2008 . Published Online: 11 November 2008

E. León-Gutierrez, G. Garcia, A. F. Lopeandía, J. Fraxedas, M. T. Clavaguera-Mora, and J. Rodríguez-Viejo



View Online



Export Citation

ARTICLES YOU MAY BE INTERESTED IN

[Influence of substrate temperature on the stability of glasses prepared by vapor deposition](#)

The Journal of Chemical Physics **127**, 154702 (2007); <https://doi.org/10.1063/1.2789438>

[Relaxation in glassforming liquids and amorphous solids](#)

Journal of Applied Physics **88**, 3113 (2000); <https://doi.org/10.1063/1.1286035>

[Glass transition and stable glass formation of tetrachloromethane](#)

The Journal of Chemical Physics **144**, 244503 (2016); <https://doi.org/10.1063/1.4954665>

The Journal
of Chemical Physics

2018 EDITORS' CHOICE

READ NOW!



In situ nanocalorimetry of thin glassy organic films

E. León-Gutiérrez,¹ G. García,¹ A. F. Lopeandía,¹ J. Fraxedas,² M. T. Clavaguera-Mora,¹ and J. Rodríguez-Viejo^{1,3,a)}¹Group of Nanomaterials and Microsystems, Department of Physics, Universitat Autònoma de Barcelona, Campus UAB, 08193 Bellaterra, Spain²Centre d' Investigació en Nanociència i Nanotecnologia, CIN2 (CSIC-ICN), Campus UAB, 08193 Bellaterra, Spain³MATGAS Research Centre, Campus UAB, 08193 Bellaterra, Spain

(Received 15 July 2008; accepted 9 October 2008; published online 11 November 2008)

In this work, we describe the design and first experimental results of a new setup that combines evaporation of liquids in ultrahigh vacuum conditions with *in situ* high sensitivity thermal characterization of thin films. Organic compounds are deposited from the vapor directly onto a liquid nitrogen cooled substrate, permitting the preparation and characterization of glassy films. The substrate consists of a microfabricated, membrane-based nanocalorimeter that permits *in situ* measurements of heat capacity under ultrafast heating rates (up to 10^5 K/s) in the temperature range of 100–300 K. Three glass forming liquids—toluene, methanol, and acetic acid—are characterized. The spikes in heat capacity related to the glass-transition temperature, the fictive temperature and, in some cases, the onset temperature of crystallization are determined for several heating rates. © 2008 American Institute of Physics. [DOI: 10.1063/1.3009766]

The glass-to-liquid transition, characterized by the glass-transition temperature T_g , is a fundamental feature of a supercooled system.^{1,2} The thermodynamics and kinetic properties of the inherently metastable glass state are of great interest both for fundamental studies as well as for a number of technological applications.³ Two approaches are typically used to prepare glasses: (1) ultrafast cooling to quench the liquid below the freezing temperature and (2) preparing amorphous films directly from the vapor phase by condensing the molecules onto a cold substrate. A glassy solid can then be heated up above its T_g to become either a supercooled liquid or a crystalline solid. Calorimetry is a standard technique to determine T_g in bulk materials, exhibiting a jump of the calorimetric signal at the transition temperatures.⁴

Literature reports on calorimetry of glassy thin films are scarce and generally based on *ex situ* experiments performed at low temperatures on glassy systems by adapting conventional differential scanning calorimetry with cryogenic vessels.⁵ Recently, the development of highly sensitive micro-machined calorimeters has allowed the study of phase transitions in thin films.^{6–8} Efremov *et al.*⁶ and Lupaşcu *et al.*,⁷ for example, have measured transitions in supported polymer thin films. The analysis of the glass transition in very thin supported films, however, even in model materials such as polystyrene, is still a matter of debate.^{9,10} As opposed to their bulk counterparts, thin films may be strongly affected by exposure to air or moisture, by the experimental conditions, and by the measurement technique. The ability to measure the glass transition without air exposure by producing and measuring samples *in situ* in an ultrahigh vacuum environment is therefore extremely important.¹⁰

Although vapor-deposited glassy samples have previously been prepared and characterized by calorimetry,^{11,12} Swallen *et al.*⁵ demonstrated only recently the higher stability of glass samples prepared from the vapor phase as compared to samples prepared by cooling the supercooled liquid.

In this work, we propose a novel setup that combines thermal evaporation in ultrahigh vacuum conditions with *in situ* high resolution measurements of the heat capacity of thin films. The method allows glass-transition analysis in glass forming liquids even for ultrathin samples.

The key advantage of this system lies in the use of micro-machined membrane-based devices that, due to their low thermal mass and small dimensions, can achieve very fast heating and cooling rates with enough sensitivity to measure phase transitions even in ultrathin films.⁶

The proposed procedure for determining glass transition and crystallization temperatures offers a number of benefits: (i) ultrahigh purity samples can be prepared from the vapor phase under UHV conditions; (ii) condensation from the vapor phase facilitates the formation of vitreous structures, unlike liquid quenching; (iii) quasiadiabatic nanocalorimetry allows for direct determination of C_p ; (iv) the large range of heating rates, reaching above 10^5 K/s, allows for kinetic measurements and a dynamic analysis of the glass transitions; (v) a single calorimeter chip can be successfully used for hundreds of successive experiments after subliming the film from the substrate; and (vi) the high sensitivity permits measurements on films as thin as a few nanometers.

In order to assess the reproducibility and limitations of the proposed methodology, we have characterized three pure organic liquids. Bulk toluene and methanol have well-known glass-transition temperatures of 117 K (Ref. 13) and 103 K (Ref. 14) respectively. Acetic acid has only recently been studied, with an estimated T_g around 130 K (Ref. 15) as

^{a)}Electronic mail: javirod@vega.uab.es.

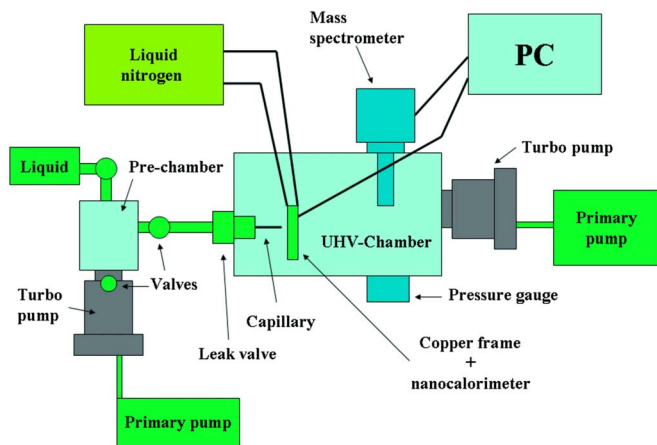


FIG. 1. (Color online) Schematic of the experimental setup.

determined by time-of-flight secondary ion mass spectrometry and temperature programmed desorption.

Commercial toluene, methanol, and acetic acid (all $\geq 99.9\%$) were purchased from Sigma-Aldrich and used as received without further purification. Each liquid is placed in a stainless steel or pyrex container followed by several freeze-pump-thaw cycles to remove dissolved gases. A schematic of the whole system is shown in Fig. 1.

After the container returns to room temperature, the vapor pressure of the sample liquid is high enough to be introduced into the UHV transfer prechamber using a needle valve. By carefully opening the high-precision leak valve connecting the prechamber with the main chamber, we control the leak rate into the main chamber and thus the quantity of vapor near the substrate. The vapor is injected through a glass microcapillary connected to the leak valve. As illustrated in Figs. 1 and 2, the end of the capillary is located 1 mm away from the cooled nanocalorimeter surface, where the vapor rapidly condenses. During this step, the composition of the gas that enters the main chamber is monitored

using a residual gas analyzer (RGA), which also permits a rough estimate of the quantity of vapor injected. Recent findings by Efremov *et al.*¹⁰ show that the presence of an RGA may modify the properties of organic films due to interaction with the radicals produced by molecules cracking on the RGA filament. We therefore carried out several tests with the RGA on and off during film growth and/or heat scans and have not observed any substantial effect on the shape or position of the glass transition. The absence of a RGA effect may be related to the ultrahigh vacuum of our system (10^{-9} mbar base pressure) and the small size of the deposition area (shown in Fig. 2).

Figure 2 shows the cross sections of the microchip holder and the microchip itself, acting as the film substrate. The microchip is sandwiched between two copper supports cooled by liquid nitrogen. The temperature of the support is monitored by a $100\ \Omega$ platinum resistive temperature sensor, PT100. The microdevices consist of a 180 nm thick SiN_x membrane suspended on a silicon frame. On top of the membrane, a platinum thin film is patterned by lift-off to define the heater and sensor elements. Details of the microfabrication process as well as of the thermomechanical stability are described elsewhere.^{16,17} As shown in Fig. 2, a shadow mask ensures selective film deposition only on the platinum heater of one of the calorimetric sensors, while the second sensor is protected from any deposition and therefore serves as a reference in the differential measurements. No changes in the Pt line resistance were observed upon deposition of the various films.

Prior to the experiments, the microchips are calibrated individually in an external cryostat and the resistance at room temperature as well as the temperature coefficient of resistance (TCR) are determined. Two almost identical nanocalorimeters are then selected and mounted on the copper holders and located in the UHV chamber, evacuated down to 10^{-9} mbar with a turbomolecular pump connected in series

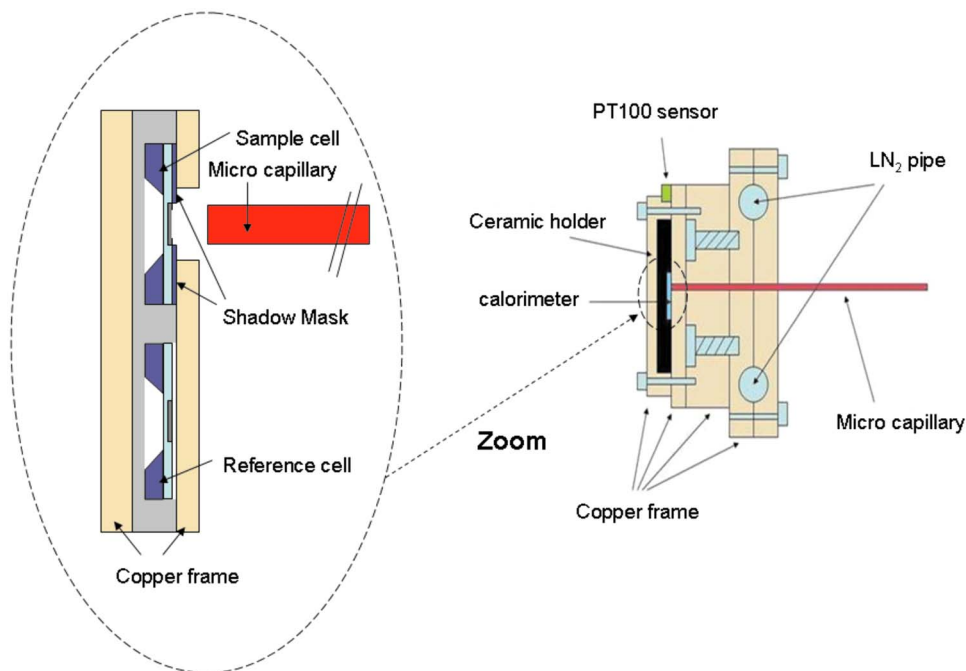


FIG. 2. (Color online) Schematics of the copper holder support (left) and cross section of the twin membrane-based nanocalorimeter system (right).

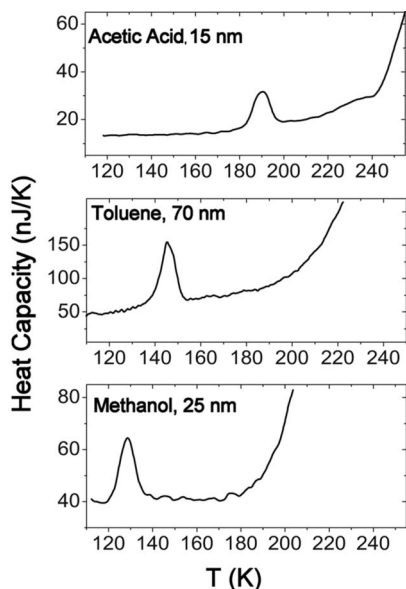


FIG. 3. Heat capacity curves obtained from the first scan after film deposition of the various glass forming liquids as a function of temperature. Curves are smoothed for clarity with a ten point adjacent averaging.

with an oil-sealed mechanical roughing pump. Before depositing the films, hundreds of calorimetric scans are performed by consecutively heating both nanocalorimeters up to 350 K and self-cooling to 80 K. This procedure determines the initial difference between the two calorimetric cells, which will be used as the baseline to be subtracted from the final measurements. After this internal calibration procedure, the selected vapor is introduced into the main chamber as described above and rapidly condenses on the nanocalorimeter surface, forming a glassy film. During deposition, the substrate is maintained at 90 K using a proportional-integral-derivative controller that controls the amount of current supplied to the Pt element of the calorimetric sensor. The temperature can thus be tuned and maintained constant to any desired value above liquid nitrogen temperature. Immediately after film deposition, scans are performed by heating the nanocalorimeter up to the desired temperature at heating rates of around 3.5×10^4 K/s. At such fast rates, the heat capacity of the sample can be evaluated from the measurement of the differential voltage between the two calorimetric cells, ΔV , as a function of time according to the expression¹⁸

$$C_p^{\text{sample}}(T(t)) = - \frac{V_R(t)}{(dT/dt)^2} \frac{d\Delta V}{(dR/dT)|_t dt}, \quad (1)$$

where $V_R(t)$ is the reference voltage at a given time and (dR/dT) accounts for the TCR of the microchips. The final C_p value is obtained after several corrections described in detail elsewhere.^{16,18} Figure 3 shows the heat capacity as a function of temperature determined from the first heat scan of the three films deposited at $T=90$ K. We observe a clear heat capacity jump at the glass transition as well as a large overshoot due to the fast heating rate. The apparent increase in heat capacity observed at higher temperatures is attributed to film desorption. We estimate the mass of the film using the experimental data and the specific heat of the bulk material at around 100 K,^{11,13,19} where the contribution of sublimation

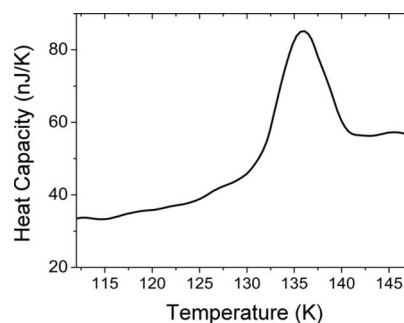


FIG. 4. Heat capacity of a toluene film (nominal thickness of around 40 nm) obtained by averaging 50 consecutive measurements under identical heating (3.5×10^4 K/s) and cooling (2×10^3 K/s) conditions.

to the heat capacity is negligible. Taking into account the deposition area and the densities of the liquids,^{20–22} we evaluate film thicknesses and growth rates. Typical growth rates are found to be around 0.01 nm/s and film thicknesses range from 15 to 70 nm. From Fig. 3 we extract the glass-transition onset temperature T_g defined by the intersection of a linear fit of the C_p in the glassy state and the rise in C_p . T_g values determined at 3.5×10^4 K/s in the first scan after film growth are 185, 139, and 119 K for acetic acid, toluene, and methanol, respectively. These values are substantially higher than those measured with conventional heating rates (≈ 1 –10 K/min) on conventional glasses: 130 (Ref. 15), 117.5 (Ref. 13) and 103 K (Ref. 14) for acetic acid, toluene, and methanol, respectively. Integration of the heat capacity yields the enthalpy upon heating and is used to obtain the fictive temperature. T_f is calculated to be 160 and 111 K for acetic acid and toluene, respectively. The T_f of methanol could not be measured accurately because it lies below the starting temperature of the calorimetric scan (around 100 K).

Limiting the final temperature to below the onset of non-reversible processes, including sublimation, ensures reproducibility and allows us to carry out many consecutive scans under identical heating and cooling rates. The data can thus be averaged and the signal-to-noise ratio of the curves improved as shown for toluene in Fig. 4. When comparing the first scan of toluene [Fig. 3(b)], corresponding to the vapor-deposited film, with the subsequent scans (Fig. 4), corresponding to fast cooling from the liquid, a significant change in both T_f and T_g is observed. The lower fictive temperature of the as-deposited sample, $T_f=111$ K, compared to $T_f=117$ K for the fast-cooled one, is indicative of its higher thermodynamic stability. Also, the as-deposited sample exhibits an enthalpy that is 3 J/g lower than the enthalpy of the fast-cooled sample. These results are in agreement with recent data from Swallen *et al.*,⁵ who first demonstrated that vapor-deposited films can be more relaxed than supercooled ones. Similarly, the lower T_g (131 K) and a substantially smaller height of the overshoot of the fast-cooled (from the liquid) sample compared to the as-deposited film ($T_g=139$ K) indicate a greater kinetic stability of the vapor-deposited sample. For toluene, we also measure the jump in heat capacity from the glass to the supercooled state, $\Delta C_p=0.35$ J/g K, which closely agrees with the bulk value of 0.37 J/g K.¹³ It is worth noting that the sensitivity of this

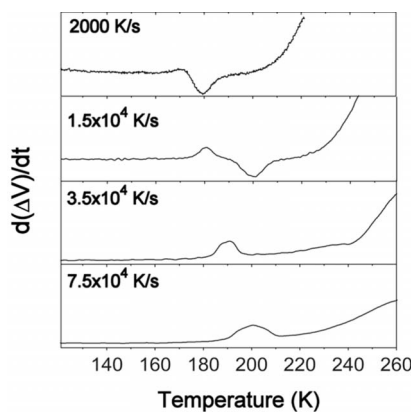


FIG. 5. Differential voltage vs temperature for glassy films of acetic acid analyzed at various heating rates.

technique is high enough to detect changes in C_p as low as a few nJ/K.

The influence of the heating rate on the phase transitions was investigated in methanol and acetic acid, both of which are expected to crystallize within the temperature range studied. For instance, at standard heating rates of few K/min, methanol readily crystallizes 3–5 K above T_g . In our case, as indicated by Fig. 3, heating of 3.5×10^4 K/s inhibited the crystallization upon heating at least in the temperature range measured. This phenomenon was expected, as crystallization kinetics typically depend more strongly on the heating rate than does the glass transition; hence a larger supercooled region may be observed at much higher heating rates.²³ The second scan does not show the presence of a glass transition, suggesting that methanol undergoes a liquid-to-crystalline transition upon the slower cooling from the liquid (at around 2000 K/s).

The effect of increasing the heating rate on the apparent heat capacity curve of an acetic acid glassy film is even more evident, as shown in Fig. 5. The curves correspond only to first scans performed just after sample deposition, varying the heating rate from 2000 to 7.5×10^4 K/s. Because at the lower scan rates the sample behaves nonadiabatically, the results of Fig. 5 are presented as $d\Delta V/dt(T)$, which contains the same temperature dependence as the heat capacity curve. The trace at 2000 K/s shows an upswing of the apparent heat capacity just before the exothermic event which indicates that crystallization ($T_x \approx 172$ K) occurs before reaching a steady supercooled liquid state. T_g was estimated to be 164 K at a heating rate of 2000 K/s. The rapid endothermic rise of the signal above 210 K is due to sublimation of the sample. Upon increasing the heating rate to 1.5×10^4 K/s, both the glass transition (175 K) and the crystallization ($T_x \approx 191$ K) events are clearly resolved due to the different activation energies of the two processes. The region between them is the supercooled liquid region, which can be expanded by using even higher heating rates (3.5×10^4 K/s) as shown in Fig. 5, where T_g was estimated in 184 K. At the highest heating rate of 7.5×10^4 K/s, T_g is determined to be 190 K, the crystallization is frustrated in the analyzed tem-

perature range and the sublimation is also retarded compared to the slower scans. The procedure used in this work could thus provide a means to explore the supercooled liquid region, between the glass transition and the crystallization, in many other materials.

In conclusion, we have shown that *in situ* nanocalorimetric measurements performed in a UHV evaporation chamber provide a unique opportunity to explore the stability of vapor-deposited glass films by measuring their heat capacity over a wide temperature range. The applicability of the technique is demonstrated by measuring the jump in heat capacity associated with the glass transition in glassy films of toluene, acetic acid, and methanol under different heating and cooling rates. *In situ* preparation and characterization are shown to be useful methods for studying the stability and aging phenomena of glassy systems. Further enhancement of the system to allow for intermediate heating and cooling rates is underway, and the results will be the subject of future work.

We acknowledge the former Ministerio de Educación y Ciencia for support through Project Nos. MAT2007–61521 and FIS2006–26391 EXPLORA and the Generalitat de Catalunya through Project No. SGR2005–00201. E.L.G. thanks MEC for FPI fellowship.

- ¹S. M. Dounce, J. Mundy, and H.-L. Dai, *J. Chem. Phys.* **126**, 191111 (2007).
- ²P. G. Debenedetti and F. H. Stillinger, *Nature (London)* **410**, 259 (2001).
- ³C. A. Angell, *Science* **267**, 1924 (1995).
- ⁴G. W. Höhne, W. F. Hemminger, and H.-J. Flammersheim, *Differential Scanning Calorimetry* (Springer-Verlag, Berlin, 2007).
- ⁵S. F. Swallen, K. L. Kearns, M. K. Mapes, Y. S. Kim, R. J. McMahon, M. D. Ediger, T. Wu, L. Yu, and S. Satija, *Science* **315**, 353 (2007).
- ⁶M. Y. Efremov, E. A. Olson, M. Zhang, Z. Zhang, and L. H. Allen, *Phys. Rev. Lett.* **91**, 085703 (2003).
- ⁷V. Lupaşcu, H. Huth, C. Schick, and M. Wübbenhorst, *Thermochim. Acta* **432**, 222 (2005).
- ⁸A. F. Lopeandía, J. Rodríguez-Viejo, M. Chacón, M. T. Clavaguera-Mora, and F. J. Muñoz, *J. Micromech. Microeng.* **16**, 965 (2006).
- ⁹Z. Fakhraai and J. A. Forrest, *Phys. Rev. Lett.* **95**, 025701 (2005).
- ¹⁰M. Y. Efremov, S. S. Soofi, A. V. Kiyanova, C. J. Munoz, P. Burgardt, F. Cerrina, and P. F. Nealey, *Rev. Sci. Instrum.* **79**, 043903 (2008).
- ¹¹M. Sugisaki, H. Suga, and S. Seki, *Bull. Chem. Soc. Jpn.* **41**, 2586 (1968).
- ¹²M. Chonde, M. Brindza, and V. Sadtschenko, *J. Chem. Phys.* **125**, 094501 (2006).
- ¹³C. Alba, L. E. Busse, D. J. List, and C. A. Angell, *J. Chem. Phys.* **92**, 617 (1990).
- ¹⁴M. Sugisaki, H. Suga, and S. Seki, *Bull. Chem. Soc. Jpn.* **40**, 2984 (1967).
- ¹⁵R. Souda, *Chem. Phys. Lett.* **413**, 171 (2005).
- ¹⁶A. F. Lopeandía, Ph.D. thesis, Universitat Autònoma de Barcelona, 2007.
- ¹⁷A. F. Lopeandía, E. León-Gutiérrez, J. Rodríguez-Viejo, and F. J. Muñoz, *Microelectron. Eng.* **84**, 1288 (2007).
- ¹⁸M. Y. Efremov, E. A. Olson, M. Zhang, S. L. Lai, F. Schiettekatte, Z. S. Zhang, and L. H. Allen, *Thermochim. Acta* **412**, 13 (2004).
- ¹⁹G. S. Parks and K. K. Kelley, *J. Am. Chem. Soc.* **47**, 2089 (1925).
- ²⁰D. Morineau, Y. Xia, and C. Alba-Simionesco, *J. Chem. Phys.* **117**, 8966 (2002).
- ²¹D. Morineau, R. Guégan, Y. Xia, and C. Alba-Simionesco, *J. Chem. Phys.* **121**, 1466 (2004).
- ²²H. Bertagnolli and H. G. Hertz, *Phys. Status Solidi A* **49**, 463 (1978).
- ²³B. Zhang, R. J. Wang, D. Q. Zhao, M. X. Pan, and W. H. Wang, *Phys. Rev. B* **70**, 224208 (2004).